24. Matthews, M. R. *et al.* Vortices in a Bose-Einstein condensate. *Phys. Rev. Lett.* **83,** 2498 (1999).
25. Hall, D. S., Matthews, M. R., Ensher, J. R., Wieman, C. E. & Cornell, E. A. Dynamics of component separation in a binary mixture of Bose-Einstein condensates. *Phys. Rev. Lett.* **81,** 1539–1542 (1998).

Acknowledgements

We thank E. A. Cornell, M. R. Matthews, P. C. Haljan, B P. Anderson and C. E. Wieman for discussions on the realization of our scheme, and R. Walser and J. Cooper for comments. This work was supported by the National Science Foundation.

Correspondence and requests for materials should be addressed to M.J.H. (e-mail: mholland@hbar.colorado.edu).

Coherent transport of electron spin in a ferromagnetically contacted carbon nanotube

Kazuhito Tsukagoshi*, Bruce W. Alphenaar† & Hiroki Ago‡

* *The Institute of Physical and Chemical Research (RIKEN), Wako, Saitama 351-0198, Japan*
† *Hitachi Cambridge Laboratory, Madingley Road, Cambridge CB3 0HE, UK*
‡ *Cavendish Laboratory, Madingley Road, Cambridge CB3 0HE, UK*

Conventional electronic devices generally utilize only the charge of conduction electrons; however, interest is growing in 'spin-electronic' devices[1], whose operation depends additionally on the electronic spin. Spin-polarized electrons (which occur naturally in ferromagnetic materials) can be injected from a ferromagnet into non-ferromagnetic materials[2–4], or through oxide tunnel barriers[3,5–10]. The electron-scattering rate at any subsequent ferromagnetic/non-ferromagnetic interface depends on the spin polarity, a property that is exploited in spin-electronic devices. The unusual conducting properties[11–18] of carbon nanotubes offer intriguing possibilities for such devices; their elastic- and phase-scattering lengths are extremely long[16,17], and carbon nanotubes can behave as one-dimensional conductors[18]. Here we report the injection of spin-polarized electrons from ferromagnetic contacts into multi-walled carbon nanotubes, finding direct evidence for coherent transport of electron spins. We observe a hysteretic magnetoresistance in several nanotubes with a maximum resistance change of 9%, from which we estimate the spin-flip scattering length to be at least 130 nm—an encouraging result for the development of practical nanotube spin-electronic devices.

Figure 1 shows the geometry of our ferromagnetically contacted nanotube devices. We use crude multi-walled carbon nanotubes (MWNTs) synthesized from graphite rods by the arc discharge evaporation method under a helium atmosphere[11]. This ensures that the MWNTs contain no trace of magnetic catalysts. The MWNTs are extracted into suspension in dichloroethane by a short sonication, and then dispersed and dried onto a SiO_2/Si substrate. We map out the MWNTs with respect to Pt/Au alignment marks on the substrate using a scanning electron microscope. (The nanotubes show no damage from low-magnification electron microscopy.) The MWNTs are typically 10–40 nm in diameter and 1 μm or more in length. Contact patterns are defined using electron beam lithography, after which a 65-nm-thick layer of Co is deposited by thermal evaporation at a pressure of 4×10^{-7} torr. The resulting polycrystalline Co film behaves ferromagnetically, and has a room-temperature resistivity of approximately 22 μΩ cm. After lift-off, the ferromagnetic leads are connected to non-ferromagnetic Cr/Au bond-pads. Figure 1a is an electron micrograph showing the junction region of a completed device. We have fabricated and characterized more than 50 such devices. Among these, the room-temperature two-terminal resistance varies between 10 and 150- kΩ. When cooled to 4.2 K, the resistance typically increases by a factor of 2–3, in agreement with recently published work[16]. The Co contacts remain ohmic up to biases of 10 mV at low temperature.

Magnetoresistance measurements are performed in a 4.2 K bath cryostat with the magnetic field (B) from a superconducting magnet directed in the plane of the substrate ($B_{\parallel}$). The two-terminal resistance is measured using an a.c. lock-in technique with an excitation voltage of 100 μV. We note that the lead resistance in our measurements is negligible (~10 Ω) compared with the MWNT resistance and the Co/MWNT contact resistance. The field is swept slowly (<10 mT min^{-1}); at this sweep rate the magnetoresistance of test samples contacted by Au/Pt shows no hysteresis in the applied field. Figure 2 shows the two-terminal differential resistance of three different Co-contacted nanotubes as a function of magnetic field. The field is swept first from −100 mT to 100 mT (solid line) and then back to −100 mT (dashed line). In each trace, a resistance peak appears as the magnetic field moves through 0 T. The width of the resistance peak is ~50 mT, which is commensurate with the coercive field strength for a thin Co film[19]. There is also a large hysteresis in the peak position (~±50 mT) between positive and negative sweep directions, indicating the probable influence of the contact magnetisation.

Similar hysteretic magnetoresistance is observed in magnetic tunnel junctions (MTJs), where it has been attributed to spin-polarized electron tunnelling[1,5–10]. MTJs consist of two ferromagnetic contacts separated by a thin oxide layer. The conduction electrons within the ferromagnetic contacts have a preferred spin direction, which is determined by the local magnetization. This causes the formation of majority and minority spin conduction bands with different densities of states at the Fermi energy. In the absence of spin-scattering, the resistance across the tunnel barrier is

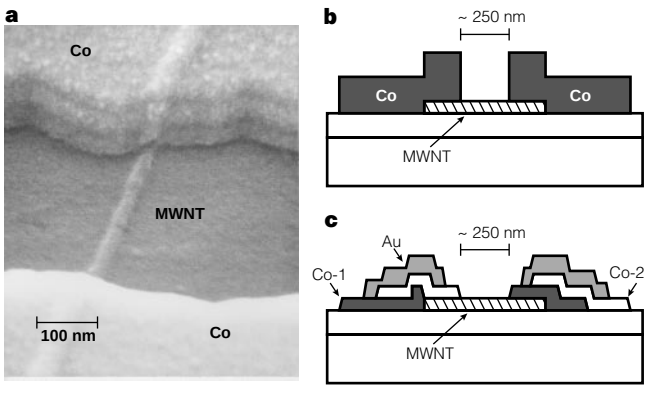

Figure 1 Structure of our devices, consisting of a single multi-walled carbon nanotube (MWNT) electrically contacted by ferromagnetic Co. **a**, Scanning electron microscope image of the device, near the Co/MWNT junction. The Co contacts lie on top of the MWNT, and the conducting channel is 250 nm in length. The image of the nanotube is seen through the Co layer, due to the change in height of the evaporated film. The diameter of this particular nanotube is 30 nm; the diameters varied from 10 to 40 nm. **b**, Schematic diagram of the device. The substrate is a semi-insulating Si wafer covered by a 200-nm-thick layer of SiO_2. The electrodes are polycrystalline Co, deposited by thermal evaporation and defined by electron beam lithography. Non-ferromagnetic leads are positioned ⩾30 μm from the MWNT. The spin polarization of the transport electrons is determined by the local magnetic domains in contact with the MWNT. **c**, Alternative device geometry resulting from a shadow evaporation technique. Note that the Au capping layer does not come in contact with the nanotube, and serves only to protect the ferromagnetic contact layer.

dependent on the relative alignment of the magnetization of the two contacts. In the anti-parallel state the majority spin states are out of alignment and the junction resistance is higher than in the parallel state in which the majority spin states are aligned.

For the nanotube devices in Fig. 2, the contact magnetizations align parallel with the magnetic field at $B = \pm 100$ mT. As we sweep B through 0 T, the magnetization polarity switches. The observed peak in the nanotube resistance suggests that the contact magnetizations switch separately and become misaligned as the field is swept. For a MTJ, misalignment occurs because different ferromagnetic contact materials are used, with different coercivities—the magnetizations are misaligned when B lies between the coercive fields of the two contacts. But this does not explain the misalignment in the nanotube device, because the average coercivity of the two Co contacts should be very similar. In this case, the misalignment may be caused by magnetization fluctuations that occur locally, on the scale of the nanotube diameter (30 nm). The average Co domain size (50 nm; ref. 19) is of the order of the width of the nanotube, so that the nanotube contacts only a small number of magnetic domains. The coercivity of each domain varies, and depends on its geometry and the local energy conditions. Edge and surface effects are also important. It is reasonable, then, that there will be a range of B over which the magnetization at the two nanotube contacts will be misaligned. A resistance peak due to the misaligned state occurs, even though the average properties of the two contacts are similar. The small switches in the resistance, seen most clearly in Fig. 2a, provide additional evidence for local magnetization fluctuations of individual domains.

In Fig. 2 we include data from three different samples to give a fair indication of the large sample-to-sample variation typically observed in the magnetoresistance. In all, 12 of our Co-contacted samples displayed hysteretic magnetoresistance, with a peak height varying from 2% to 10%. Two samples showed a step-like resistance peak as seen in Fig. 2a, while the remaining samples showed a smoother peak as seen in Figs 2b and c. It is likely that the sample-to-sample variations are due to inherent random variations in the surface potential over the small nanotube contact area. Previous experiments on non-magnetically contacted nanotubes have observed large variations in the contact resistance[12,16]. Also, in the ferromagnetically contacted samples it is impossible to control the particular domain structure in contact with the nanotube. Reproducibility might be improved by increasing the thickness and quality of the Co layers, which will increase the area of the magnetic domains. Unfortunately, our maximum film thickness (and hence the domain width) is limited to ~100 nm by the electron-beam lithographic procedure.

The spin-injection model for the nanotube magnetoresistance requires a sufficiently small amount of spin scattering to occur both within the nanotube, and at the interfaces between the nanotube and the contacts. We can estimate the minimum spin-scattering length in the MWNT using Julliere's model for the MTJ. The difference between the tunnel resistance in the parallel (R_p) and antiparallel (R_a) states[5] is given by:

$$\Delta R/R_a = (R_a - R_p)/R_a = 2P_1P_2/(1 + P_1P_2)$$

Here, P_1 and P_2 are the percentage of conduction electrons polarized in the majority spin band in the ferromagnetic contacts 1 and 2. For Co, the polarization has been determined[8] to be 34% giving a maximum resistance change of 21%. In our best case, $\Delta R/R_a$ reaches a maximum value of 9% (Fig. 2b) so that ~14% of the spin-polarized electrons travel the 250 nm through the nanotube without spin-flipping. The spin-scattering length, l_s, can then be estimated by assuming that the spin polarization reduces as $\exp(-l/l_s)$ within the nanotube. This gives $l_s = 130$ nm. Although fairly long, this is probably an underestimation. The spin-polarization near the ferromagnet/nanotube interface will depend on the interface quality, and could be appreciably lower than 34%. Also, we do not take into account spin scattering at the ferromagnet/nanotube interface. Finally, we note that the MTJ theory cannot be expected to completely describe our carbon nanotube device, and a more exact theoretical description is needed.

In an effort to improve the reproducibility of the Co/nanotube contacts, we have fabricated a set of devices using a double evaporation technique (Fig. 1c). Cobalt is evaporated from either side of the substrate to create a continuous Co layer over the nanotube. A gold capping layer is then evaporated from directly

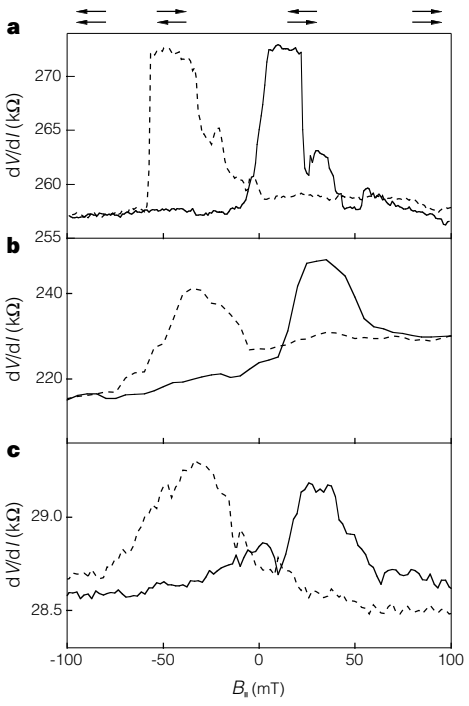

Figure 2 Two-terminal differential resistance as a function of magnetic field for three different MWNT devices. The magnetic field $B_\parallel$ is directed parallel to the substrate, and the temperature is 4.2 K. The solid (dashed) trace corresponds to the positive (negative) sweep direction. The differential resistance shows a large variation among devices—the device shown in **c** has a resistance an order of magnitude lower than the devices shown in **a** and **b**. This is probably due to variations in the contact resistance. The two-terminal resistance could sometimes be lowered by thermal annealing. Each device shows a large hysteretic magnetoresistance peak. We attribute the magnetoresistance peak to spin-polarized injection[1,5–10] between the ferromagnetic contacts and the MWNT. The magnetization direction of the left and right contacts is represented by the direction of the arrows at the top of the figure. When the magnetizations of the two contacts are parallel, the resistance is lower than when the magnetization of the two contacts are antiparallel. This explanation requires that the spin scattering length in the nanotube is of the order of the contact separation. Also, scattering at the contact interfaces must not completely randomise the spin. The percent difference $\Delta R/R_a$ between the tunnel resistance in the parallel and the antiparallel states is approximately 6% in **a**, 9% in **b** and 2% in **c**.

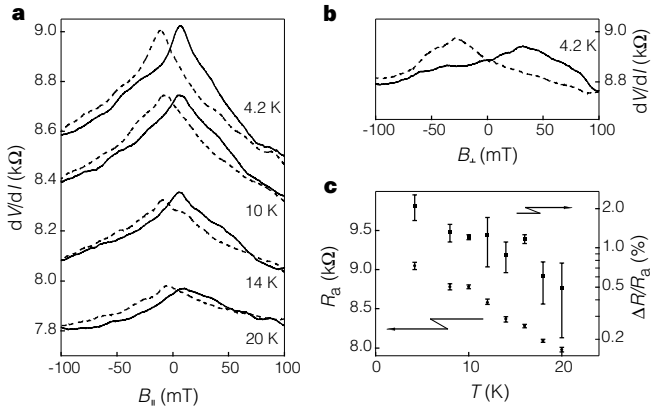

Figure 3 Detailed characterization of a single nanotube device. This device was fabricated using a shadow evaporation technique, resulting in the geometry shown in Fig. 1c. Note that the resistance, magnetoresistance ratio and coercive field are all less than for the devices shown in Fig. 2. **a**, The temperature dependence of the magnetoresistance for magnetic field directed parallel to the substrate ($B_\parallel$). The solid (dashed) trace corresponds to the positive (negative) sweep direction. The magnetoresistance ratio $\Delta R/R_a$ decreases approximately exponentially with increasing temperature, but the peak positions remain at a fixed value of $B_\parallel$. **b**, The magnetoresistance for field directed perpendicular to the substrate ($B_\perp$). The increase in the peak positions and the decrease in the peak heights indicates the presence of an anisotropic domain structure. **c**, The magnetoresistance ratio $\Delta R/R_a$ and R_a for the data set shown in **a**. The error bars take into account the different peak resistance values in the two sweep directions. $\Delta R/R_a$ increases approximately exponentially with decreasing T, while R_a increases approximately linearly.

above the substrate to protect the Co surface. Figure 3a shows the magnetoresistance of a nanotube contacted with a double Co layer as a function of $B_\parallel$. This technique improves the continuity of the Co film, and reduces the contact resistance in comparison with the single-Co-layer devices. However, the magnetoresistance ratio $\Delta R/R_a$ and the coercive field are both less than in Fig. 2. Also, rather than observing a sharp magnetoresistance peak, the magnetic field dependence is continuous, similar to what is observed in a granular ferromagnetic film[20]. This implies that the magnetization is averaged over many small magnetic domains in the double layer Co devices, each with relatively weak coercivities. This averaging improves the stability of the contact, but unfortunately also lowers the magnetoresistance ratio. Figure 3b shows the magnetoresistance as a function of B perpendicular to the substrate ($B_\perp$) for the same sample. The peaks are broader and shifted to higher fields when compared with the $B_\parallel$ dependence. This is expected for a ferromagnetic film with an in-plane easy axis of magnetization[6].

The temperature dependence in Fig. 3a shows that the percentage difference between the resistance in the parallel and antiparallel configurations goes to zero as the temperature increases from 4.2 to 20 K. In Fig. 3c we see that $\Delta R/R_a$ decreases approximately exponentially with increasing temperature. The exact mechanism for the temperature dependence is not yet known. Given the low atomic number of carbon, the spin–orbit scattering in the carbon nanotube (and hence its temperature dependence) should be negligible. However, the spin polarization at the interface will decrease with increasing temperature if the nanotube/ferromagnet interface is of relatively poor quality[8–10]. In addition, the effective contact area will increase with temperature, resulting in the averaging of the spin polarization over a increasing number of magnetic domains. We anticipate that $\Delta R/R_a$ should also decrease with increasing bias across the device, as a similar effect is observed in spin-tunnel junctions[6]. However, our nanotube devices do not survive biases above ~10 mV; breakdown occurs before any appreciable change in $\Delta R/R_a$ is observed. Finally, using the double evaporation technique, we have also made a set of devices having two contacts made from different materials, NiFe and Ni. Hysteretic magnetoresistance is observed, with $\Delta R/R_a \approx 2\%$ at 4.2 K.

The results presented here are consistent with recent experiments that show that the electron path lengths within MWNTs are extremely long. The phase coherence length has been found to be 250 nm, and the elastic scattering length 60 nm[16]. Further work has shown that MWNTs behave as ballistic conductors, even at room temperature[18]. We expect that the spin-flip scattering in the nanotubes should also be highly suppressed. Consider, for example, that the spin scattering length in a metal[4] or a semiconductor[21] is typically much longer than the phase coherence length or the elastic scattering length. This has allowed progress on a new generation of functional devices whose operation is based on both the charge and spin of the electron ('magnetoelectronics')[1]. Although we are still some way from producing a practical nanotube spin-electronic device, improvements in the sample preparation should allow the observation of larger and cleaner spin-modulated resistances. Our technique also opens up the possibility of studying magnetically contacted single-walled nanotubes, which could reveal the influence of spin injection on the spin polarization of the carbon nanotube[22,23]. □

Received 6 May; accepted 2 August 1999.

1. Prinz, G. A. Magnetoelectronics. *Science* **282,** 1660–1663 (1998).
2. Tedrow, P. M. & Meservey, R. Spin-dependent tunnelling into ferromagnetic nickel. *Phys. Rev. Lett.* **26,** 192–195 (1971).
3. Aronov, A. G. Spin injection in metals and polarisation of nuclei. *Pis'ma Zh. Eksp. Teor. Fiz.* **24,** 37–39 (1976); *JETP Lett.* **24,** 32–34 (1976).
4. Johnson, M. & Silsbee, R. H. Interfacial charge-spin coupling–injection and detection of spin. *Phys. Rev. Lett.* **55,** 1790–1793 (1985).
5. Julliere, M. Tunnelling between ferromagnetic films. *Phys. Lett. A* **54,** 225–226 (1975).
6. Moodera, J. S. *et al.* Large magnetoresistance at room temperature in ferromagnetic thin film tunnel junctions. *Phys. Rev. Lett.* **74,** 3273–3276 (1995).
7. Miyazaki, T. & Tezuka, N. Giant magnetic tunnelling effect in Fe/Al_2O_3/Fe junction. *J. Magn. Magn. Mater.* **139,** L231–L234 (1995).
8. Meservey, R. & Tedrow, P. M. Spin-polarised electron tunnelling. *Phys. Rep.* **238,** 173–243 (1994).
9. Moodera, J. S., Nowak, J. & van de Veerdonk, R. J. M. Interface magnetism and spin wave scattering in ferromagnet-insulator-ferromagnet tunnel junctions. *Phys. Rev. Lett.* **80,** 2941–2944 (1998).
10. Shang, C. H., Nowak, J., Jansen, R. & Moodera, J. S. Temperature dependence of magnetoresistance and surface magnetization in ferromagnetic tunnel junctions. *Phys. Rev. B* **58,** R2917–R2920 (1998).
11. Ebbesen, T. W. & Ajayan, P. M. Large-scale synthesis of carbon nanotubes. *Nature* **358,** 220–222 (1992).
12. Langer, L. *et al.* Quantum transport in multiwalled carbon nanotubes. *Phys. Rev. Lett.* **76,** 479–482 (1996).
13. Dai, H., Wong, E. W. & Lieber, C. M. Probing electrical transport in nanomaterials: conductivity of individual carbon nanotubes. *Science* **272,** 523–526 (1996).
14. Ebbesen, T. W. *et al.* Electrical conductivity of individual carbon nanotubes. *Nature* **382,** 54–56 (1996).
15. Saito, R., Dresselhaus, G. & Dresselhaus, M. S. *Physical Properties of Carbon Nanotubes* (Imperial College Press, Singapore, 1998).
16. Bachtold, A. *et al.* in *Proc. 12th Int. Winter School on Electronic Properties of Novel Materials* (eds Kuzmany, H., Fink, J., Mehring, M. & Roth, S.) 65–68 (Am. Inst. Phys., New York, 1998).
17. Bachtold, A. *et al.* Aharonov-Bohm oscillations in carbon nanotubes. *Nature* **397,** 673–675 (1999).
18. Frank, S. *et al.* Carbon nanotube quantum resistors. *Science* **280,** 1744–1746 (1998).
19. Rüdiger, U. *et al.* Magnetoresistance, micromagnetism, and domain-wall scattering in epitaxial hcp Co films. *Phys. Rev. B* **59,** 11914–11918 (1999).
20. Chien, C. L. Magnetism and giant magneto-transport properties in granular solids. *Annu. Rev. Mater. Sci.* **25,** 129–160 (1995).
21. Kikkawa, J. M. & Awschalom, D. D. Resonant spin amplification in n-type GaAs. *Phys. Rev. Lett.* **80,** 4313–4316 (1998).
22. Cobden, D. H. *et al.* Spin splitting and even-odd effects in carbon nanotubes. *Phys. Rev. Lett.* **81,** 681–684 (1998).
23. Tans, S. J. *et al.* Electron-electron correlations in carbon nanotubes. *Nature* **394,** 761–764 (1998).

Acknowledgements

We thank H. Mizuta, T. Nakanishi, M. D. R. Thomas, D. G. Hasko and H. O. Müller for discussions.

Correspondence and requests for materials should be addressed to B.W.A. (alphenaar@ phy.cam.ac.uk).